

Evidence for water influx from a caldera lake during the explosive hydromagmatic eruption of 1790, Kilauea volcano, Hawaii

Larry G. Mastin

Cascades Volcano Observatory, U.S. Geological Survey, Vancouver, Washington

Abstract. In 1790 a major hydromagmatic eruption at the summit of Kilauea volcano, Hawaii, deposited up to 10 m of pyroclastic fall and surge deposits and killed several dozen Hawaiian natives who were crossing the island. Previous studies have hypothesized that the explosivity of this eruption was due to the influx of groundwater into the conduit and mixing of the groundwater with ascending magma. This study proposes that surface water, not groundwater, was the agent responsible for the explosiveness of the eruption. That is, a lake or pond may have existed in the caldera in 1790 and explosions may have taken place when magma ascended into the lake from below. That assertion is based on two lines of evidence: (1) high vesicularity (averaging 73% of more than 3000 lapilli) and high vesicle number density (10^5 – 10^7 cm⁻³ melt) of pumice clasts suggest that some phases of the eruption involved vigorous, sustained magma ascent; and (2) numerical calculations suggest that under most circumstances, hydrostatic pressure would not be sufficient to drive water into the eruptive conduit during vigorous magma ascent unless the water table were above the ground surface. These results are supported by historical data on the rate of infilling of the caldera floor during the early 1800s. When extrapolated back to 1790, they suggest that the caldera floor was below the water table.

Introduction

In the early 1800s the first European visitors to Kilauea volcano were told of an eruption decades earlier that had devastated the summit and decimated a Hawaiian army that was crossing the island. By Hawaiian standards the eruption was so large and violent that survivors recalled the details some 50 years later [Dibble, 1843]. Eyewitnesses described “pillars” of glowing ash, viewed from the northwest end of the island, that towered over Mauna Loa, some 9 km above their Kilauea vent [Jaggard, 1921]. Survivors who were passing near the crater described [Dibble, 1843, pp. 52–55] “A dense cloud of darkness [that rose] out of the crater, . . . [and] continued to ascend and spread abroad until the whole region was enveloped and the light of day was entirely excluded . . . Soon followed an immense volume of sand and cinders which were thrown in high heaven and came down in a destructive shower for many miles around.” Several members of one group and all members of a second group, some 80 to a few hundred by various accounts [Ellis, 1827, p. 174; Hitchcock, 1909, p. 166], were killed. A future eruption of this type would pose a greater hazard to human life than any recent volcanic activity in Hawaii.

Beginning in the late 1800s [Dana, 1888], the explosiveness of the 1790 eruption was attributed to water that entered the conduit. Studies in the 1970s and 1980s confirmed this suspicion by describing surge beds, fine average grain size, accretionary lapilli, and other classic hydromagmatic features in the deposit [Swanson and Christiansen, 1973; Christiansen, 1979; Decker and Christiansen, 1984; McPhie et al., 1990]. There is no longer much doubt that water was responsible for the violence

of the eruption. Still uncertain, however, are the exact circumstances that allowed it to mix with magma. The prevailing hypothesis has been that groundwater, rather than surface water, was involved. In this study I raise a mechanical consideration that points toward a different water source.

The consideration is that in order for groundwater to enter the conduit, the pressure of magma and gases in the conduit must be less than the pressure of the surrounding groundwater. This condition may be easily satisfied during certain phases of an eruption, during eruptive pauses, for example, when magma draws down below the water table. However, during vigorous magma ejection, conduit pressures should be very high; water should enter the conduit under these conditions only if its pressure is higher still. This issue applies to all hydromagmatic eruptions, though its importance is rarely mentioned. With regard to Kilauea this study focuses on three questions: (1) did the eruption of 1790 involve water/magma mixing during vigorous magma ascent? (2) If so, what conduit pressures might have existed during those conditions? Finally, (3) how could water pressures have exceeded the magma pressure and entered the conduit?

Keanakakoi Deposit

The deposit produced in 1790, known as the Keanakakoi Ash [Wentworth, 1938; Easton, 1987], blankets the ground within several kilometers of the caldera rim (Figure 1). It lies directly over a nonhydromagmatic layer of reticulite and pumice (unit I of Decker and Christiansen [1984]) (Figure 2) that was produced during high lava fountains [Christiansen, 1979; Decker and Christiansen, 1984; McPhie et al., 1990]. The reticulite eruption was followed by a pause of sufficient duration to allow minor reworking of the deposit but not long enough for soil or vegetation to develop.

This paper is not subject to U.S. copyright. Published in 1997 by the American Geophysical Union.

Paper number 97JB01426.

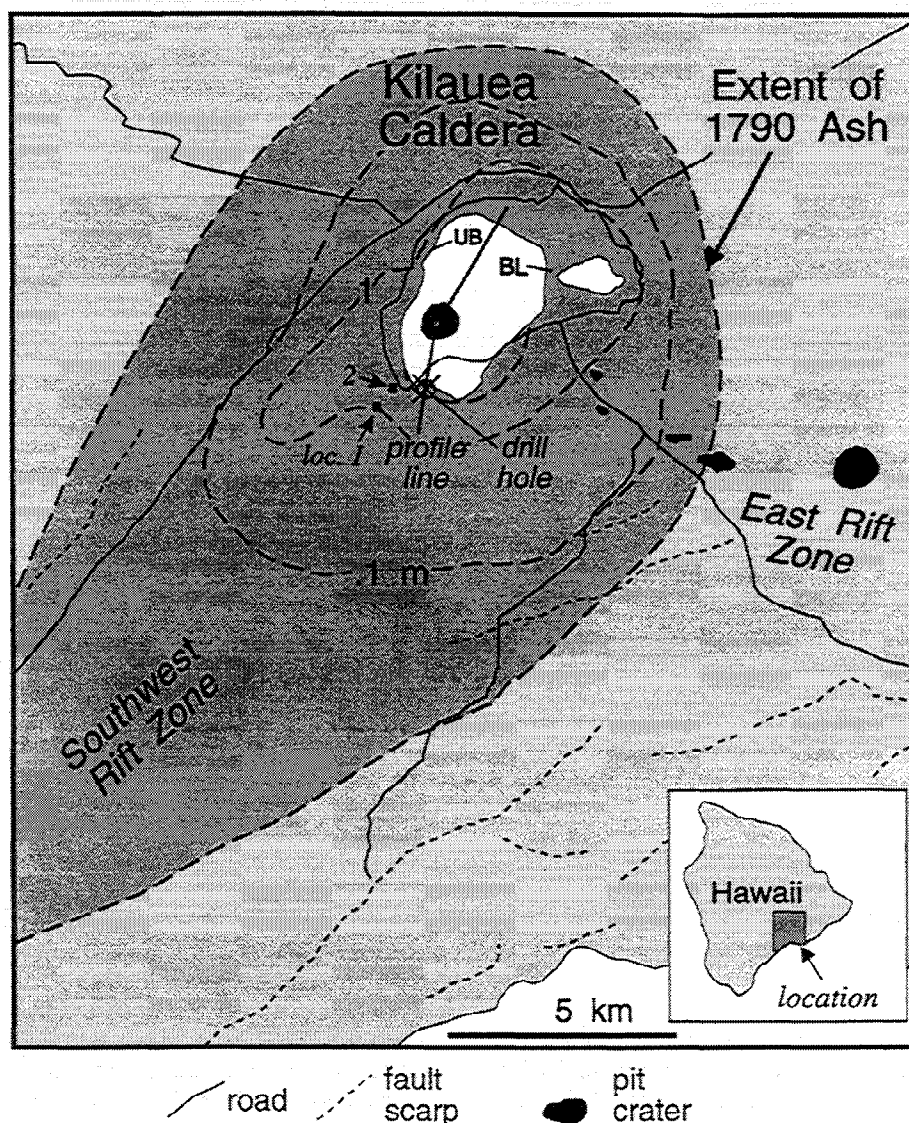


Figure 1. Kilauea Caldera and surrounding area, showing thickness distribution of the Keanakakoi Ash (long-dashed lines) as mapped by *Stearns and Clark* [1930]. The profile line shows the location of the cross section illustrated in Figure 11. Locations 1 and 2 are sites where juvenile lapilli fragments were collected from the unit II deposit. BL is Byron Ledge and UB is Uwekahuna Bluff.

The lowermost unit of the Keanakakoi Ash proper (unit II of *Decker and Christiansen* [1984] and units 1–4 of *McPhie et al.* [1990]) contains well-bedded fall and low-energy surge beds composed almost entirely of juvenile ash and lapilli. The fine average grain size and presence of accretionary lapilli (among other features) indicate that all units from the main vent mixed with water [*McPhie et al.*, 1990]. (Unit IIC2 in Figure 2 is not hydromagmatic, but it erupted from a source southeast of the main caldera vent.) The paucity of lithic debris has been interpreted to indicate a high magma/water ratio and relatively stable vent walls during this part of the eruption [*Christiansen*, 1979; *Decker and Christiansen*, 1984; *McPhie et al.*, 1990].

Overlying unit II and separated from it by a major surge unconformity is a heterogeneously distributed member (unit III of *Decker and Christiansen* [1984] and units 5–10 of *McPhie et al.* [1990]) containing roughly equal proportions of lithic debris and fine-grained juvenile ash. Extensive cross-bedded surge deposits, abundant lithic fragments, local accretionary

lapilli, and major surge erosion suggest that this phase produced large, discrete explosions combined with vent wall erosion or collapse. Locally, overlying this member near the southwest rim of the caldera are deposits of lava, Pele's hair, and Pele's tears (unit IV of *Decker and Christiansen* [1984]) from an eruption through a fissure circumferential to the caldera's southwest margin.

The uppermost member (unit V of *Decker and Christiansen* [1984] and units 11–16 of *McPhie et al.* [1990]) consists of lithic debris ejected as ballistic fragments or incorporated into fall and surge beds. The predominance of lithic fragments suggests that this stage was driven by massive vent wall collapse and by contact of hot country rock with inflowing water. The uppermost lithic unit is overlain by a nonhydromagmatic pumice and reticulite deposit (unit VI of *Decker and Christiansen* [1984]) on the western sector of the caldera. It was designated the "golden pumice" by *Sharp et al.* [1987] and hypothesized by them to have erupted in the early 1800s.

Previous Interpretations

Christiansen [1979] and *Decker and Christiansen* [1984] interpreted the Keanakakoi sequence as follows: (1) The magma column initially stood high in Kilauea, erupting very high lava fountains and depositing the basal reticulite layer. (2) Rapid lowering of the magma column, perhaps related to an eruption recorded in about 1790 on Kilauea's lower east rift zone or to submarine eruptions, allowed groundwater to enter magmatic conduits beneath the summit area. Contact of water with magma caused hydromagmatic eruptions and produced fall deposits and planar-bedded surges. (3) As the magma level continued to drop, more water entered and explosions became more intense; progressively, more lithic material erupted with the vitric ash, and surge-flow deposition became greatly predominant; with summit deflation (subsidence), magma from an isolated shallow storage chamber was able to erupt a small flow through a circumferential fracture. (4) As magma dropped below the level of the explosions, only lithic ash and blocks erupted, commonly in surge flows; major caldera subsidence followed. (5) Ultimately, magma returned to a high level and erupted lava fountains in the caldera.

McPhie et al. [1990] suggested a similar sequence of events. Their study differed from that of *Decker and Christiansen* [1984] mainly in their emphasis on certain features, specifically (1) the importance of vesiculation and degassing as fragmentation processes early in the eruption; (2) the possible evidence for pauses of weeks or months between eruptive stages; and (3) the historical evidence that the caldera floor may have been 300–500 m deeper in 1790 than today. But their fundamental interpretation, like that of the earlier authors, involved draw-down of magma in the conduit by flank eruptions and increasing influx of groundwater during the course of the eruption.

Problems With Previous Interpretations

In interpreting the lowermost, juvenile-rich member of the Keanakakoi Ash, *McPhie et al.* [1990] envisioned eruptive pulses that were caused by fluctuations in the elevation of the magma column in the conduit, with pulses produced when gas-rich magma rose through degassed liquid and mixed with inflowing groundwater. *McPhie et al.* [1990, p. 351] stated that

“Hundreds of explosions are recorded by the lower division clearly repeating a definite pattern, such as (a) rising of the magma in the conduit in response to buildup of volatile pressure; (b) vesiculation and partial fragmentation of the magma; (c) mixing of the variably vesiculated fragments with water and/or steam at the level of the aquifer; (d) steam- and volatile-driven explosive eruption of the thoroughly fragmented, mostly juvenile ejecta; (e) deflation and subsidence of the remaining degassed magma below the site of interaction with water, resetting conditions favorable to (a).”

Although some layers of the unit II deposit do contain alternating beds of ash and lapilli, it is not clear that each layer represents a separate eruptive pulse. On weathered surfaces (Figure 3, right), layers a few millimeters to centimeters thick are inconspicuous and defined by subtle variations in grain size. Most contacts are gradational, not sharp as might be expected if pulses were separated by pauses or surge erosion. The variations in grain size between layers could be related to temporal changes in the magma/water ratio, in the magma supply rate, or in the wind direction as well as to discrete explosive pulses.

McPhie et al. [1990] also suggest that the volume of each

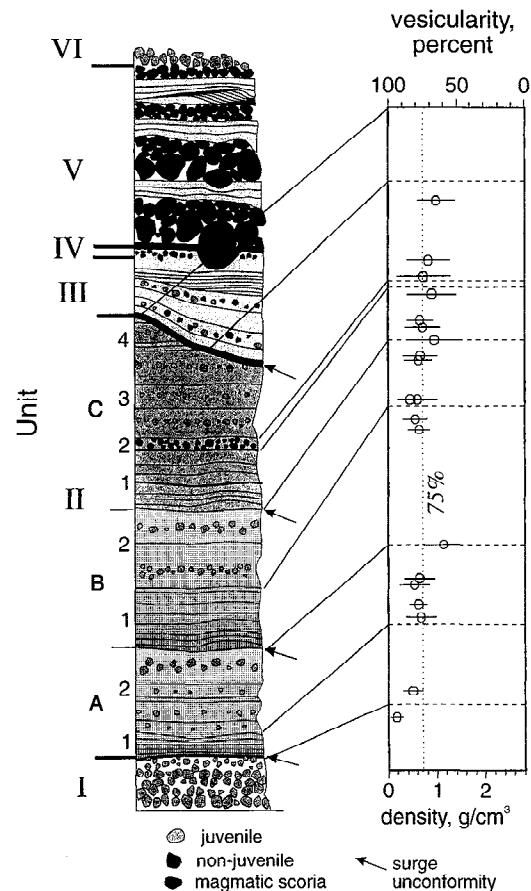


Figure 2. (left) Schematic columnar section of the Keanakakoi Ash. Stratigraphic nomenclature taken from *Decker and Christiansen* [1984]. (right) Average density and vesicularity of lapilli in coarse-grained horizons. Each circle represents the mean of 100–130 lapilli fragments, and the length of each solid bar encompasses the standard deviation on each side of the mean.

eruptive pulse was small, resulting from fluctuations in the magma level in the conduit of perhaps only a few meters. Indeed, under their scenario the pulses would have to have been small; otherwise, the magma would have risen to a level above the water table during each pulse, making it difficult for water to enter. Yet some characteristics suggest that the deposit was produced by sustained pulses. The lowermost two thirds of unit II, for example, consist of two well-defined beds of fine ash that grade upward into coarse lapilli (Figures 2 and 3, units IIA and IIB). These fine-coarse sequences are separated from one another and from the overlying beds by erosional surge contacts which represent the only widespread unconformities in the unit II deposit [*Decker and Christiansen*, 1984]. The sequences contain no internal structures (such as rainwash gullies or soil deposits) that would argue against their deposition in single, semicontinuous eruptive pulses. Isopach thicknesses [from *McPhie et al.*, 1990; L. G. Mastin, unpublished data, 1996] suggest that each sequence contains of the order of a hundredth of a cubic kilometer of dense rock magma, thousands of times more than would occupy the uppermost hundred meters of a 10-m-diameter conduit.

If each sequence were, in fact, generated by numerous small pulses, many thousands would be required (each representing about a 10-m rise in the conduit magma level) to account for

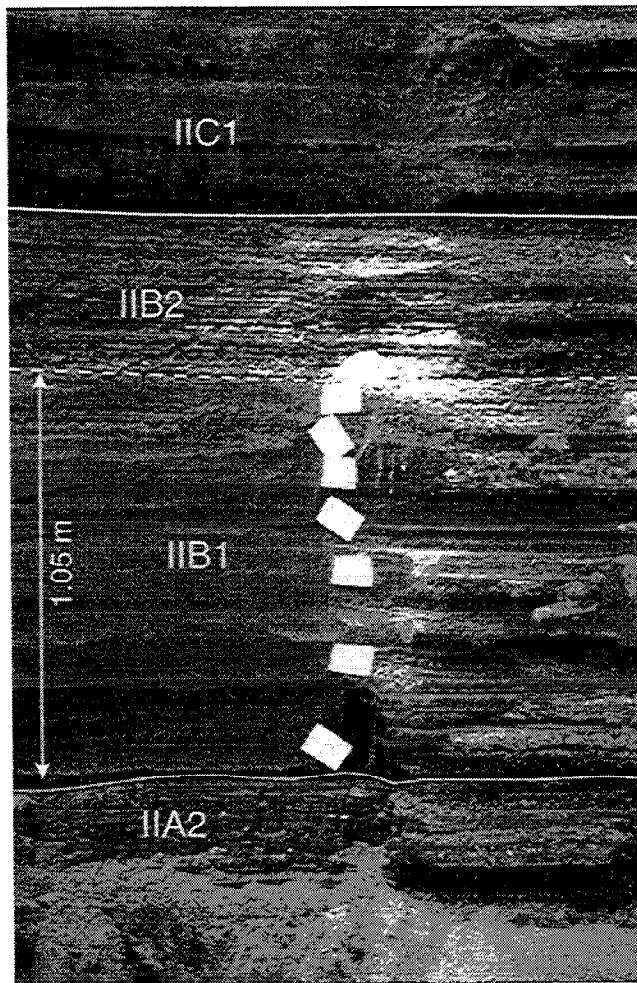


Figure 3. Outcrop photograph of unit IIB from Sand Wash (Figure 1, location 2). The left side of the outcrop was smoothed with a shovel; the right side still displays the weathered texture.

their volume. If each pulse were separated by tens of minutes, the activity would have had to continue unabated for years. On the other hand, if the sequences were generated by fewer pulses of larger volume, it seems unavoidable that during some pulses, magma would have filled the conduit, excluding the entrance of additional groundwater and generating interbeds of nonhydromagmatic lava-fountain tephra. (Some pulses could perhaps have produced intracaldera lava flows which are no longer preserved. However, one would still expect at least some nonhydromagmatic lava-fountain tephra if there had been any significant nonhydromagmatic eruptive pulses.) With the exception of one layer (unit IIC2) which originates from a different eruptive center than all other units, no nonhydromagmatic horizons exist in the deposit.

A second characteristic that suggests sustained eruptive pulses is the abundance of highly vesiculated pumice in units IIA2 and IIB2. The pumice fragments are remarkable for their abundant, very fine textured vesicles (Figure 4). Quantitative studies at Kilauea [e.g., Mangan *et al.*, 1993; Cashman *et al.*, 1994; Mangan and Cashman, 1996] show that highly vesiculated, fine-textured pumice is produced only in lava fountains which involve sustained, high rates of magma flux. This point was also recognized by Dvorak [1992], though he made no

actual studies of clast vesicularity to compare with other Kilauean deposits. Here I attempt such a study.

Pumice Vesicularity

To study pumice vesicularity, more than 3000 juvenile lapilli were collected from the unit II deposit at two well-exposed sections (Figure 1, locations 1 and 2). The lapilli were obtained from all horizons where a statistically significant number (considered somewhat arbitrarily to be 100–130) could be removed by sieving at the outcrop. Following Houghton and Wilson [1989], densities were measured by drying them, spraying them with a hydrophobic silicon compound that prevented penetration of water into the vesicles, and then weighing each clast in and out of water.

Vesicle size distributions were measured by M. T. Mangan (U.S. Geological Survey (USGS), Hawaiian Volcano Observatory (HVO), unpublished data, 1995) in four clasts from unit IIB2 (Figure 2). On the basis of visual inspection the vesicle size and abundance in those clasts appear to be typical of other Keanakakoi pumice. Methods of analysis are described in Mangan *et al.* [1993]. The size distribution studies were undertaken primarily to quantify the vesicle number density, a measure of the number of vesicles per cubic centimeter of melt.

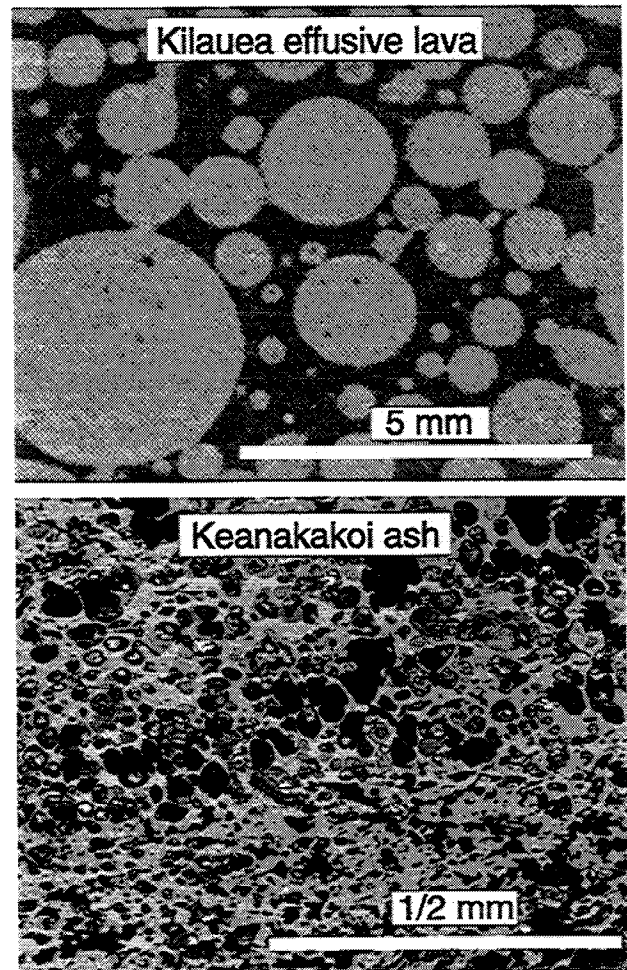


Figure 4. Typical bubble size and abundance (top) in Kilauea effusive lava [from Mangan *et al.*, 1993] and (bottom) in a pumice lapillus from unit IIB2. Note the difference in scale between the two photos.

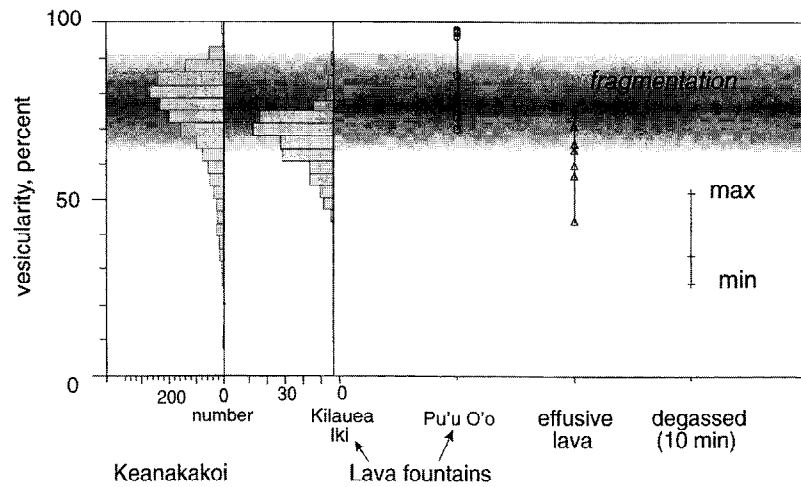


Figure 5. Vesicularity of lava sampled from different types of eruptions at Kilauea volcano. Vesicularity data for juvenile Keanakakoi lapilli are from this study. The source of data for Kilauea Iki is *Houghton and Wilson* [1989], for Pu'u O'o is *Mangan and Cashman* [1996], for effusive lava is *Mangan et al.* [1993], and for degassing is *Cashman et al.* [1994]. Dark band represents zone of fragmentation, centered approximately at 75% vesicularity.

Results

The clast density measurements (Figures 2 and 5) confirm that vesicularity of the lapilli is both high (the average for all clasts is 73%) and remarkably uniform (standard deviation is 12%). Fewer than 2% of lapilli contain vesicularities lower than 40%. This lies within the range of vesicularities of most lava-fountain tephra (Figure 5). It exceeds the vesicularity of most, but not all, effusive lava collected at eruptive vents (40%–75% [*Mangan et al.*, 1993], occasionally, up to 85% (M. Mangan, personal communication, 1996)) and is clearly greater than Kilauean lavas that have degassed even for only several minutes (20%–40% [*Cashman et al.*, 1994]).

The vesicle size analyses (Figure 6) give number densities (~10⁵–10⁷ vesicles cm⁻³) that exceed not only those of typical effusive lavas (10³–10⁴ vesicles cm⁻³ [*Mangan et al.*, 1993]) but also of tephra from lava-fountain eruptions in the twentieth century (10⁴–10⁵ [*Mangan and Cashman*, 1996]). Dominant

diameters of the Keanakakoi vesicles are 0.03–0.07 mm, smaller than those of both historic Pu'u O'o lava-fountain tephra (0.1–0.2 mm [*Mangan and Cashman*, 1996]) and effusive lavas (0.2–0.4 mm [*Mangan et al.*, 1993]).

Significance of Vesicularity

It is generally assumed that vigorous lava fountains are produced by gas-rich magma, whereas mild, effusive flows are produced by gas-poor magma. At Kilauea, however, effusive lava flows and fountains studied during the 1980s were both produced by magma of more or less the same initial volatile content [*Parfitt et al.*, 1995]. The style of those eruptions, whether high fountains or mild effusive flows, was determined more by the magma flux rate than by differences in volatile content. Moreover, the greater vesicularity of lava-fountain tephra was due not to higher initial magma-gas content but to the fact that during fountaining, volatiles exsolved rapidly and the magma quenched quickly before gas could escape. Vesicularities in the Keanakakoi tephra may be high for the same reason, though (unlike recent historical eruptions) high initial volatile contents may also have played a role.

The high vesicle number density of the Keanakakoi tephra is a much stronger indicator of high magma ascent rate than vesicularity. High number density is a direct indicator of vesicle nucleation rate, which is controlled by the degree of volatile supersaturation [*Mangan and Cashman*, 1996]. The degree of supersaturation is controlled by the rate of pressure drop, which in turn is related to ascent rate. Unlike total vesicularity, vesicle number density is independent of the initial volatile content of the magma. The extreme number densities of the Keanakakoi pumice suggest unusually high rates of magma ascent.

The highest magma ascent rates are caused by forced convection of magma from a high-pressure near-surface magma chamber. Those conditions sustain vigorous fountains for hours until the pressure in the source area has been depleted. In contrast, buoyant rise of isolated packets of gas-rich magma (suggested by *McPhie et al.* [1990] for the 1790 eruption) should produce slower ascent rates and lower number densities.

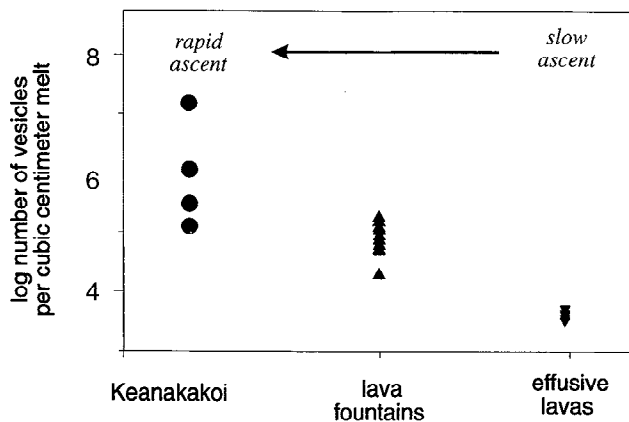


Figure 6. Number density of vesicles from lapilli in the Keanakakoi Ash, from tephra produced in Pu'u O'o lava-fountain eruptions, and from lava fragments collected at the vent during effusive eruptions at Kilauea. The source of data for lava fountains is *Mangan and Cashman* [1996] and for effusive lavas is *Mangan et al.* [1993].

If these vesicularity relationships can be applied to the Keanakakoi unit IIA2–IIB2 tephra, then one must consider it to be the product of vigorous, sustained eruption, rather than of numerous, small pulses. Magma flux during these phases would have been comparable to, or higher than, that in lava fountains during historic time, and the term “fountaining” is used in this paper to describe it (though whether these hydromagmatic eruptions actually “fountained” is unclear). The only conceivable alternative explanation for the high number densities is that vesiculation took place very rapidly during the impulsive decompression that follows discrete hydromagmatic explosions. This explanation is not considered very likely; tephra produced during discrete hydromagmatic explosions in historic time has generally been of moderate or low vesicularity (e.g., Ukinrek Maars [Kienle *et al.*, 1980] and surge beds at Surtsey [Heiken and Wohletz, 1985, pp. 85–90]). Although well-vesiculated hydromagmatic deposits have been reported (e.g., Mayor Island and Lake Taupo, New Zealand [Houghton and Wilson, 1989]), it is not clear whether they were produced during discrete explosions or sustained eruptions. From a theoretical standpoint the steam that drives hydromagmatic explosions comes from the quenching of magma early in the explosion process. Decompression that could drive vesiculation takes place late in the explosion after a large fraction of magma has already been quenched.

If water flowed into the eruptive conduit during vigorous, sustained magma ascent, it could have done so only if its pressure were higher than that of the magma and gas that occupied the conduit. In the next section I investigate what those pressures might have been.

Evolution of Conduit Pressure During an Eruption

To illustrate how conduit pressures might evolve during an eruption, consider the following idealized eruption cycle (Figure 7). Between eruptions (Figure 7a) the conduit is occupied by a static magma column, perhaps capped by fallback or collapsed vent walls near the surface (not shown). Because of its low viscosity, Kilauean magma that is exposed to atmospheric pressure loses most of its gas in a few hours [Cashman *et al.*, 1994] and should be mostly degassed in the uppermost few hundred meters between eruptions. Its density would be roughly 2650 kg m^{-3} (the density of unvesiculated magma) (Table 1) or a large fraction thereof, and the pressure in the conduit would be essentially equal to the weight of this magma (Figure 7a, dashed line). Because the magma's density is greater than that of water, its pressure at all depths will be greater than the hydrostatic pressure (Figure 7a, light solid line) unless the level of magma in the conduit drops below the water table.

Upflow of magma begins when the pressure at the base of the conduit exceeds the weight of the static magma column (Figure 7a, bold solid line). If the base of the conduit is well connected with a large magma chamber, this pressure should remain high until a large amount of magma has been expelled and the eruption has begun to wane (Figure 7e and later). As undegassed magma enters the conduit and rises, it begins to vesiculate, reducing the bulk density of the magma and hence reducing the pressure gradient (Figure 7b). As long as the pressure at the base of the conduit remains roughly constant, the conduit pressure will increase in the depth range now occupied by vesiculated magma (Figure 7b, arrows). As the

magma rises, magma pressures will increase at successively higher points in the conduit (Figure 7c, arrows). By the time the degassed plug of old magma has been completely expelled from the vent (Figure 7d), vesiculated magma would have decreased pressure gradients and hence increased subsurface conduit pressures throughout nearly the length of the conduit. (As described later, this pressure increase is reduced somewhat by frictional pressure losses as the magma begins to flow. However, for Kilauean basalt, viscosity is so low ($\sim 40\text{--}100 \text{ Pa s}$) [Ryan and Blevins, 1987] that the frictional increase in pressure gradient is small compared to the decrease resulting from vesiculation. Conduit geometry also affects the pressure gradient, as described later.)

By the time steady state lava fountaining has been achieved (Figure 7d), conduit pressures have reached their maximum. The pressure increases in the shallow conduit will cause the erupting mixture to accelerate until it reaches sonic velocities. The flow velocity can never exceed the sonic velocity except at the conduit exit or above a constriction near the exit where the conduit walls begin to flare outward. This is a basic tenet of compressible fluid flow [Liepmann and Roshko, 1957, p. 127; Wilson *et al.*, 1980]. Flows that reach sonic velocities in conduits or nozzles are said to be “choked” (Figure 7d). On the basis of modeling described in this paper and Mastin [1995], Kilauean magma-gas mixtures reach choked flow conditions at velocities of about $40\text{--}60 \text{ m s}^{-1}$, which roughly correspond to observed lava-fountain velocities (M. Mangan, USGS, HVO, personal communication, 1995). Under choked flow conditions the transition from high pressure in the subsurface to atmospheric pressure at the exit may be accomplished in at least three ways: (1) by influx of dense, degassed magma that has ponded near the vent [Wilson *et al.*, 1995], (2) by expansion and decompression of the magma-gas mixture in a flaring conduit [Wilson and Head, 1981], or (3) by abrupt decompression through shock waves at the surface, if the magma-gas mixture exceeds sonic velocity above the exit [Wilson and Head, 1981; Woods and Bower, 1995].

Toward the end of the eruption, as the pressure in the magma source area drops, the pressure throughout the conduit diminishes toward that of a vesiculated static magma column (Figure 7c). Conduit pressures reach their minimum at this point in the eruption cycle. This decrease may allow degassed magma that has accumulated around the vent to flow back in or conduit walls to collapse into the vent. Very low magma ascent rates ($< \sim 0.01 \text{ m s}^{-1}$) [Parfit and Wilson, 1995] will allow gas bubbles to coalesce, rise through the magma, and escape, increasing the overall density and pressure gradient of the remaining, degassed magma. A Hawaiian lava-fountain eruption therefore usually ends when dense, degassed magma drains back into the upper conduit, mixing with bubbly magma whose pressure is insufficient to drive it to the surface (Figure 7f). If water pressure in the host rock follows a hydrostatic curve, water will most likely enter the conduit at two points in the eruption cycle: (1) between eruptions (Figure 7a), when the static magma column drops below the water table, or (2) during the waning stages of the eruption (Figure 7c), when the open vent is occupied by highly vesiculated magma of low density.

Numerical Model

To calculate conduit pressure during an eruption, I use a numerical model for steady state, equilibrium flow of a mag-

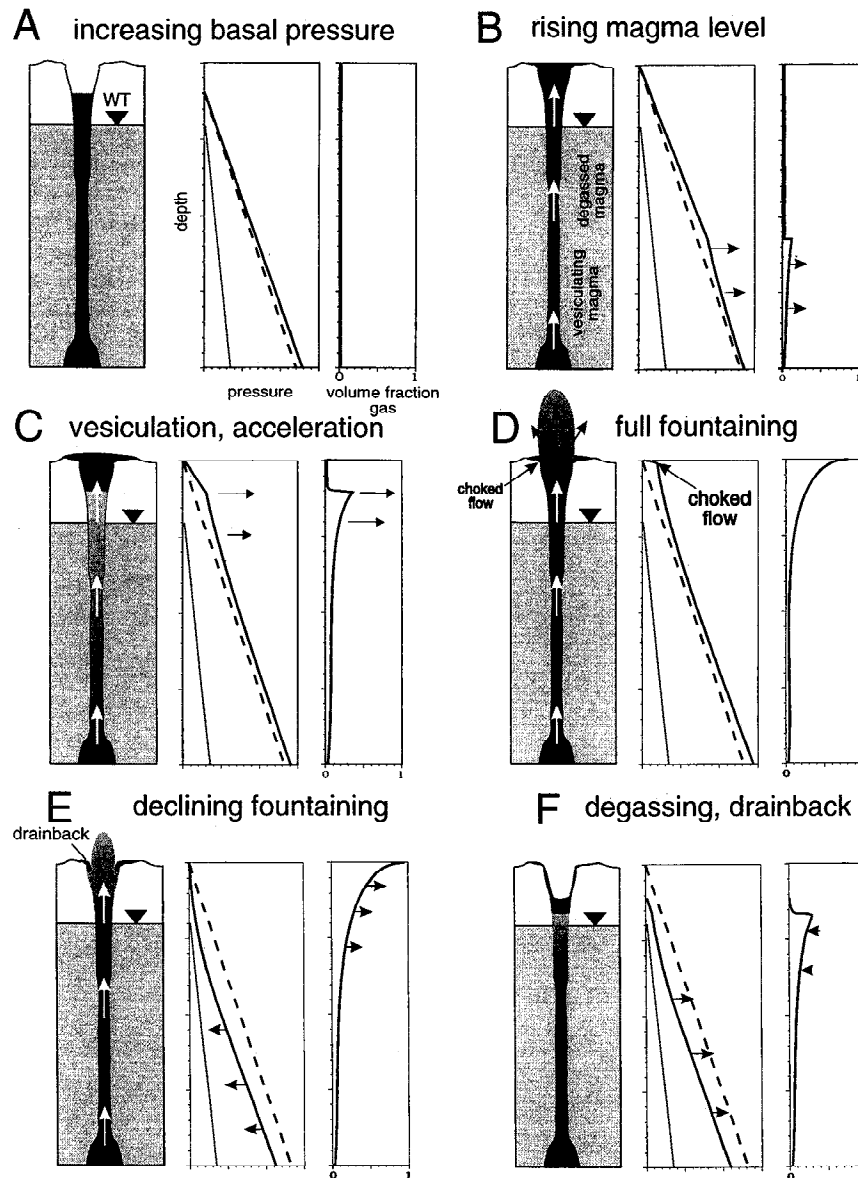


Figure 7. Evolution of pressure in an eruptive conduit at various stages of an eruptive cycle. Bold solid lines indicate pressure of magma and entrained gas. Bold dashed lines give the pressure profile of a static, degassed magma column. Light solid lines give normal hydrostatic pressure. WT is the water table. Arrows denote the change in pressure or volume fraction gas with time.

ma-gas mixture through a vertical conduit [Mastin, 1995]. A key assumption of the model is that flow of the mixture is homogeneous; that is, there is no relative movement between the gas and liquid phases. Although some researchers have argued against using this assumption when modeling basaltic eruptions [Vergnolle and Jaupart, 1986], it seems reasonable in this case. Average measured bubble diameters in the Keanakakoi are hundredths of a millimeter, and their rise velocity through magma (10^{-7} – 10^{-5} m s $^{-1}$, using Stokes flow calculations) is tiny compared to that of the magma (of the order of 1 m s $^{-1}$ or greater). Wilson *et al.* [1995] also conclude that the assumption is valid in Hawaiian eruptions when (un-vesiculated) magma ascent velocities are greater than several hundredths of a meter per second, which is the case here. If the assumption is not correct, the model would tend to underestimate pressure gradients [Dobran, 1992], giving lower conduit pressures for a given exit pressure (e.g., 1 atm) than is actually the case.

The model also assumes that gas phases (H $_2$ O, CO $_2$, and sulfur species) exsolve under equilibrium conditions, following solubility laws developed by Gerlach [1986] for Kilauean magmas, until the magma reaches the point of fragmentation (assumed to be at 75% vesicularity). Beyond that point, gas exsolution is no longer calculated, under the assumption that it does not keep pace with rates of decompression. Other assumptions are that (1) the conduit is vertical; (2) the gas phase behaves as an ideal gas; (3) the flow is steady state; (4) flow properties can be averaged across a given cross-sectional area; and (5) no heat or gas is transferred across the conduit walls.

Governing Equations

The model is derived from the equations for conservation of mass

$$\frac{d\rho}{\rho} + \frac{dv}{v} + \frac{dA}{A} = 0 \quad (1)$$

and momentum

$$-dp = \left(\rho g + \frac{f}{r} \rho v^2 \right) dz + \rho v dv \quad (2)$$

of the magma-gas mixture. The variables ρ , v , and p are the density, velocity, and pressure of the mixture, respectively, and A is the conduit's cross-sectional area. The f is a factor whose value controls frictional pressure loss in the vent [Bird *et al.*, 1960, p. 183–187], r is the radius of the conduit, g is the gravitational acceleration, and z is the vertical position (the upward direction being positive). (Because of a difference in the definition of f , the friction factor defined by Bird *et al.* [1960], used here, differs by a factor of 4 from that defined by Schlichting [1979, p. 86] and used by Wilson *et al.* [1980]. Therefore the second term in (4) also differs from the corresponding term in (1) of Wilson *et al.* [1980].)

By rearranging (1) as $dv = -v(d\rho/\rho + dA/A)$, substituting this into the right-hand term on the right side of (2), and rearranging, the following new equation is obtained:

$$-\frac{dp}{dz} \left(1 - v^2 \frac{d\rho}{dp} \right) = \rho \left(g + \frac{fv^2}{r} - \frac{v^2 dA}{A dz} \right) \quad (3)$$

This equation is made more tractable by assuming that the term $d\rho/dp$ is approximately equal to $(\partial\rho/\partial p)_s$, the partial of density with pressure under constant entropy for the erupting mixture. The latter term is the squared reciprocal of the sound speed of the mixture, c [Liepmann and Roshko, 1957, p. 50], and its value can be easily calculated. Equation 3 can therefore be rewritten as

$$\frac{dp}{dz} = \frac{\rho g + \rho v^2 \frac{f}{r} - \frac{\rho v^2 dA}{A dz}}{1 - M^2} \quad (4)$$

where M is the Mach number of the mixture, i.e., its velocity divided by its sonic velocity.

Constitutive Relationships

The following constitutive relationships are used to evaluate the terms on the right-hand side of (4). Detailed derivations of these terms are provided in Mastin [1995].

Density. The density ρ of the mixture is calculated from the equation

$$\frac{1}{\rho} = \sum \frac{m_i}{\rho_i} \quad (5)$$

where m_i and ρ_i are mass fractions and densities of the four components of the mixture: magma and the exsolved gases H₂O, CO₂, and S (actually SO₂ + H₂S). The mass fractions of each component are calculated from the gas exsolution laws of Gerlach [1986], and the densities of the gas components are taken from ideal gas relations. The density of the liquid magma is specified as input.

Friction factor. Following previous eruption modellers [Wilson *et al.*, 1980; Giberti and Wilson, 1990; Dobran, 1992], I calculate the friction factor f using an equation that sums a friction term associated with wall roughness f_o with one that depends on the Reynolds number for flow (Re):

$$f = \frac{16}{Re} + f_o = \frac{16\eta}{\rho v D} + f_o \quad (6)$$

where D is the conduit diameter and η is the viscosity of the erupting mixture. The variable f_o is empirically derived; D is specified as input; and the velocity v is calculated from the mass conservation equation, $m = \rho v A = \text{const}$, where m is the mass flux through a given cross section.

Viscosity. Unvesiculated Kilauean magma has a viscosity η_m that varies inversely with temperature in a manner approximated by the following formula [Ryan and Blevins, 1987]:

$$\log(\eta_m) = -10.737 + 1.8183 \left(\frac{10,000}{T_K} \right) \quad (7)$$

where viscosity is in Pascal seconds and T_K is temperature in kelvin (as distinguished from T_C , which is temperature in Celsius). For $T_C = 1180^\circ\text{C}$ used in this study, $\eta_m = 60$ Pa s. The numerical program estimates temperature drop during ascent from adiabatic expansion and adjusts the viscosity to take cooling into account. The amount of cooling is generally less than 15° , and the associated viscosity increases by less than about 15 Pa s.

Once gases begin to exsolve, there is little agreement on how rheology varies with vesicularity [Stein and Spera, 1992]. For Hawaiian eruptions, however, the conduit pressure profile is not very sensitive to different viscosity/vesicularity relationships [Mastin, 1995]. The relationship in this model was taken from Dobran [1992] and simplified for the case where the gas viscosity η_g is insignificant compared to that of the liquid magma η_m :

$$\eta = \frac{\eta_m}{1 - \phi} \quad \phi \leq 0.75 \quad (8a)$$

$$\eta = \eta_g \left[1 - \frac{1 - \phi}{0.62} \right]^{-1.56} \quad \phi > 0.75 \quad (8b)$$

The model calculates a gradual transition in viscosity between about $\phi = 0.7$ and $\phi = 0.8$ (where ϕ is the volume of gas divided by the total volume).

Mach Number. The Mach number of the mixture is its velocity divided by the mixture's (approximate) sonic velocity c . The latter can be calculated as

$$c = \sqrt{\frac{B}{\rho}} \quad (9)$$

where B is the bulk modulus of the mixture. For a dispersed mixture of particles in gas the bulk modulus is

$$\frac{1}{B} = \frac{v_m}{B_m} + \frac{v_{\text{H}_2\text{O}}}{B_{\text{H}_2\text{O}}} + \frac{v_{\text{CO}_2}}{B_{\text{CO}_2}} + \frac{v_S}{B_S} \quad (10)$$

where v_m , $v_{\text{H}_2\text{O}}$, v_{CO_2} , and v_S are the volume fractions of magma, water vapor, CO₂, and sulfur species exsolved, respectively, and B_m , $B_{\text{H}_2\text{O}}$, B_{CO_2} , and B_S are their bulk moduli, respectively. The bulk modulus of unvesiculated magma is of the order of 10^5 MPa [Jaeger and Cook, 1979], while bulk moduli of each gas species can be calculated from ideal gas relations (see Mastin [1995] for details).

Numerical Procedure

By specifying p , v , D , dA/dz , and other parameters listed in Table 1 at a given location (z_o) in the conduit all other terms

Table 1. Input Parameters to the Model

Parameter	Value	Comments
ρ_m	2650 kg m ⁻³	Density calculated for magma of Kilauean composition using formulas in <i>Bottinga et al.</i> [1982].
T_o	1180°C	Estimated from the average MgO content (8.35 wt%) of 230 microprobe analyses of Keanakaoi glass (L. G. Mastin and M. Beeson, unpublished data, 1995), using the chemical geothermometer of <i>Ilel and Thornber</i> [1987]. Under minimum choked flow conditions, temperatures ranging from 1150–1250°C change the water table depth required for influx by only about 18 m.
H ₂ O	0.30 wt% ^a 0.27 wt% ^b 0.27 wt% ^c	Three scenarios were used. The rationale for the choice of gas content in each scenario is explained in the text.
CO ₂	0.65 wt% ^a 0.05 wt% ^b 0.23 wt% ^c	same as above
S	0.13 wt% ^a 0.07 wt% ^b 0.11 wt% ^c	same as above
D	10 m	This value was chosen somewhat arbitrarily. Model runs have found that, under minimum choked flow conditions, variations in D from 3 to 20 m change the water table depth required for influx by only about 12 m. Smaller conduit diameters produce higher subsurface pressures, requiring shallow water tables for groundwater influx.
z_o	1 km	The variable z_o may represent the elevation of the base of the conduit or some arbitrary elevation within the conduit at which calculations begin. Thus variations in its value do not significantly affect the results.
f_o	0.0025	Typical for rough walled cylindrical conduits [<i>Bird et al.</i> , 1960]. Under minimum choked flow, variations in f_o from 0.001–0.02 change the water table depth required for influx by less than 5 m.

^aThe gas content inferred by *Gerlach and Graeber* [1985] for the shallow summit reservoir.

^bThe gas content of parent magma from the mantle, inferred by *Gerlach and Graeber* [1985].

^cAn intermediate gas content.

on the right-hand side of 4 can be determined. The pressure gradient is then calculated and a new pressure extrapolated to a higher point. The continuity and momentum equations (equations (1)–(2)) and the constitutive relations (equations (5)–(10)) are then used to evaluate flow properties and the pressure gradient at the new position. The procedure is repeated to the top of the conduit using a fourth-order Runge-Kutta integration method [*Press et al.*, 1986, p. 550]. The vertical step size is adjusted automatically to concentrate calculations at points where properties change rapidly [*Press et al.*, 1986, p. 554].

The model was tested against results of one other numerical model [*Wilson and Head*, 1981] and against two special cases for which analytical solutions exist: (1) laminar flow of a single-phase, incompressible Newtonian fluid in a vent of constant cross-sectional area and (2) flow of an ideal gas through a frictionless nozzle. Specifics of these comparisons are provided in *Mastin* [1995].

Boundary and Input Conditions

In running the model an input pressure is specified at z_o . The model then adjusts the velocity at that point until one of two exit boundary conditions are satisfied: (1) the exit pressure equals 1 atm if the exit velocity is less than sonic, or (2) the exit velocity equals the sonic velocity of the mixture. If the input pressure at depth is insufficient to drive the magma to the surface, the model stops midway through the integration process with an error message.

The values of input parameters are listed in Table 1 along with an explanation of each value chosen. Because the exact geometry of the conduit is unknown, I assume the simplest geometry, a conduit of constant cross-sectional area. The effect of other conduit geometries is discussed later.

The amounts of H₂O, CO₂, and sulfur species in the melt could not be well constrained using chemical data. I have therefore run the model using three initial volatile contents: (1) the gas content inferred by *Gerlach and Graeber* [1985] for

the shallow summit reservoir, (2) the gas content of parent magma from the mantle, inferred by *Gerlach and Graeber* [1985], and (3) an intermediate gas content.

Results

Figure 8 shows the pressure, Mach number, volume/fraction gas, and velocity of the gas-liquid mixture as a function of depth in the conduit. The dotted lines give the depth profiles in a static magma column having a volatile content corresponding to scenario 3, in which gas has exsolved to the point of equilibrium with the local pressure. The resulting vesicularities near the surface (98% at 1 atm pressure, for example) are much too high to be sustained in a static magma column. These calculations therefore give a minimum pressure that might exist in a magma column, perhaps an unrealistically low minimum.

Conduit Pressures During Fountaining

The solid lines on Figure 8 (left) define pressure profiles in a conduit whose pressure at 1-km depth is equal to the weight of a static, completely degassed magma column (26.5 MPa). These pressures would exist during full fountaining if (1) the conduit were filled with completely degassed magma before the eruption started and (2) the pressure at 1-km depth did not diminish after the eruption began. Because those conditions are not always met, these pressures are probably somewhat higher than would be expected during normal lava fountaining.

At the other end of the spectrum the dashed line on Figure 8 (left) defines the lowest conduit pressures that will produce sonic exit velocities for a magma with a gas content given by scenario 3. Because sonic velocities of the erupting mixture (40–60 m s⁻¹, calculated from the model) are approximately equal to exit velocities measured in Hawaiian lava fountains (M. Mangan, USGS, personal communication, 1995), this profile is close to the minimum that will exist during fountaining. Vent wall collapse and drainback would tend to fill in the conduit and shut off the eruption before pressures dropped

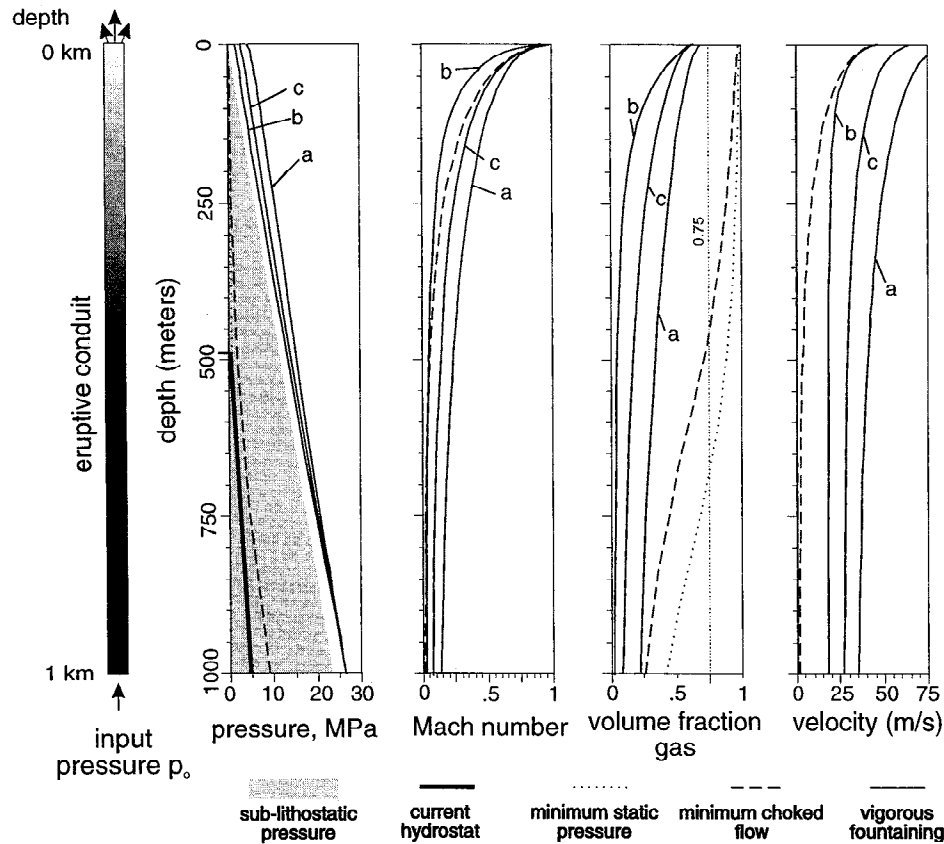


Figure 8. Pressure, Mach number, volume fraction gas, and eruptive velocity versus depth in the uppermost kilometer of an eruptive conduit. The light solid lines give depth profiles when the pressure at 1 km depth is equal to the weight of an unvesiculated magma column (26.5 MPa). Lines labeled “a,” “b,” and “c” correspond to scenarios 1, 2, and 3 in the text. The dashed line gives depth profiles for scenario 3 when the pressure at the base of the conduit is the minimum required to produce choked flow at the exit. The dotted line represents scenario 3 for a static, vesiculated magma column. The heavy solid line on the pressure plot gives the approximate, present-day hydrostat at the summit of Kilauea. Mach number and velocity under the minimum static pressure scenario are negligible and therefore do not show up on the plots.

this low. Thus these pressures would be achieved, if at all, only near the end of fountaining in a conduit with stable walls and with no ponded magma around the vent at the surface.

Water Table Depths Required for Groundwater Influx

For a given conduit pressure profile the water table depth required to drive water into the conduit can be estimated by drawing a hydrostatic pressure curve that is just tangent to the conduit pressure curve in Figure 8 and determining the depth at which it reaches $p = 1$ atm. (Such a calculation assumes, of course, that groundwater pressures follow a normal hydrostat). For the minimum choked flow condition (dashed line) this yields a water table depth of 305 m, about 180 m shallower than the present depth below the caldera floor [Keller *et al.*, 1979]. As the conduit pressure rises, the required water table depth must also rise. The middle curve in Figure 9 illustrates the water table depth required for groundwater influx under scenario 3 for conduit pressures at 1-km depth that range from the minimum required for choked flow (9.05 MPa, denoted by the arrow) to 26.5 MPa, i.e., the pressure range expected during most fountaining eruptions. Throughout more than half of this range (~ 16 –26.5 MPa) the water table would have to be above the ground surface in order to drive water into the conduit.

Effects of Input Parameters

A systematic sensitivity analysis reveals that variations in initial temperature, wall roughness, conduit diameter, conduit length, and magma density produce small to insignificant

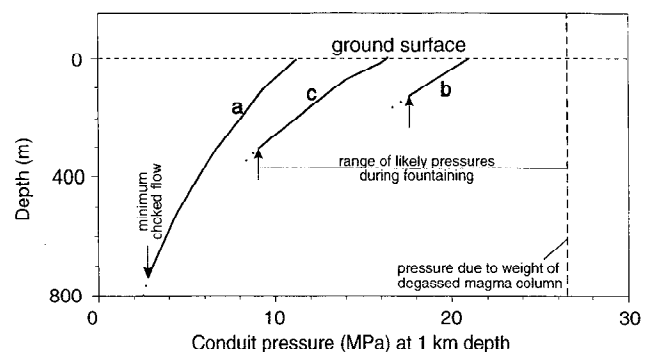


Figure 9. Water table depth required for influx of groundwater into the conduit as a function of the pressure at the base of conduit (1-km depth) during the eruption. The labels a, b, and c refer to scenarios 1, 2, and 3, respectively, in the text. The lines are dashed at pressures less than those required for minimum choked flow because the assumptions of the model begin to break down below that point.

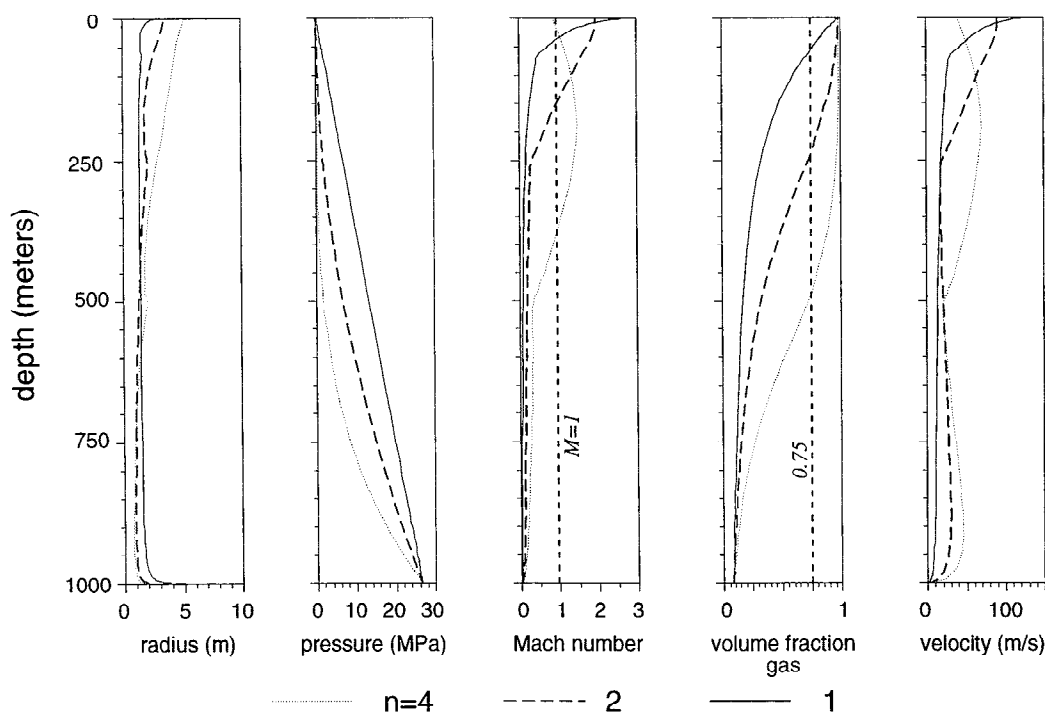


Figure 10. Conduit radius, pressure, Mach number, volume fraction gas, and velocity versus depth for the three scenarios described in the text. In each case the conduit pressure profile was specified, and the model calculated the conduit geometry that produced that profile. The parameters used as input to this model are given in Table 1.

changes in the results (Table 1). The greatest influence is provided by two input parameters: initial volatile content and conduit geometry.

Initial volatile content. Figures 8 and 9 illustrate the effect of changing magma-gas content on conduit pressures and water influx. Magma with a higher gas content (Figure 8, curve a) would exsolve greater amounts of gas at a given depth, decreasing the bulk density of the magma-gas mixture and hence decreasing the pressure gradient in the conduit. Assuming that the pressure at depth remains constant, the lower pressure gradient means that the pressure at the surface will be greater, making it more difficult for water to enter. As the eruption wanes, however, conduit pressures will drop toward those of a static magma-gas column with a constant pressure ($p = 1$ atm) at the surface. Thus the lower pressure gradient will produce lower conduit pressures at depth while still producing choked flow near the surface. For gas-rich magma, groundwater influx might be more favored during the waning stages of fountaining but less favored during peak fountaining. The opposite is true for gas-poor magmas. Neither increasing nor decreasing magma-gas content would promote water influx during all stages of fountaining.

Conduit geometry. During vigorous fountaining a conduit of constant cross-sectional area will produce pressures in the shallow subsurface that exceed lithostatic pressure, while near the end of an eruption pressures will drop below lithostatic pressure. In general, changes in conduit geometry minimize these deviations from lithostatic pressure. Slumping during low pressure will constrict the conduit, increasing the pressure at depth, while hydraulic fracturing during high pressure will enlarge the conduit, relieving overpressure [Wilson *et al.*, 1980]. Because these adjustments move the conduit pressure closer to the lithostat and because lithostatic pressure is usually at least

twice hydrostatic pressure, these change will prevent water influx.

Could a strangely shaped conduit with unusually strong walls produce subhydrostatic pressures during vigorous fountaining? Under some circumstances it could. In fact, one can “design” a low-pressure conduit by rearranging (4) to isolate the term that defines the gradient in cross-sectional area, dA/dz .

$$\frac{dA}{dz} = \frac{A}{\rho v^2} \left[\frac{dp}{dz} (1 - M^2) + \rho g + \rho v^2 \frac{f}{r} \right] \quad (11)$$

By specifying the value of dp/dz this equation can be solved for dA/dz in a manner exactly analogous to that of (4). One must specify a conduit diameter at the base of the section and an input velocity as well as the other parameters given in Table 1. Details of this procedure are explained in Mastin [1995].

Using the familiar input conditions for scenario 3, Figure 10 illustrates the conduit geometry that will produce three specified pressure profiles, each given by the equation

$$p = p_f + (p_o - p_f) \left[\frac{(z - z_f)}{(z_o - z_f)} \right]^n \quad (12)$$

where p is the pressure at a given elevation z and the subscripts f and o denote the final and initial values at the top and base of the conduit section, respectively. The exponent n can be adjusted to give different rates of pressure drop (in Figure 10, values are 1, 2, and 4). The pressure gradient at any depth is determined by differentiating (12):

$$\frac{dp}{dz} = n(p_o - p_f) \frac{(z - z_f)^{n-1}}{(z_o - z_f)^n} \quad (13)$$

Figure 10 shows that a high-pressure gradient near the base of the conduit can be produced by constricting the vent in that

area, and a lower-pressure gradient near the surface can be produced by allowing the conduit walls to flare outward. Several modeling runs have found that the specified pressure drop can be increased only to about $n = 4$ (Figure 10, dotted line). For higher values of n the conduit must flare to unrealistically high levels in the subsurface (producing a conduit hundreds or thousands of meters in diameter). For the greatest value of n that generates an acceptable solution a water table depth of about 400 m will produce groundwater influx.

There are several problems with the idea that an unusual conduit geometry may have allowed groundwater influx during active fountaining. One is that each geometry produces the specified pressure profile only under certain flow conditions. Near the beginning of an eruption, when velocities are small and the upper part of the conduit is still occupied by degassed magma, the pressure will approximate the static weight of the poorly vesiculated magma regardless of conduit geometry. The pressure in the conduit will evolve toward one shown in Figure 10 only after gas-poor magma has been expelled from the conduit.

At best this exercise suggests that at some point during vigorous fountaining, if the conduit geometry were just right, pressures could be significantly lower than they would be in a conduit of constant cross-sectional area. However, for the mechanical reasons outlined above, there is no reason to expect a conduit to evolve to such a shape. If the conduit did evolve to such a shape by some unforeseen mechanism, its walls would have to be unusually strong to prevent collapse, and ponds of degassed lava at the surface (which would fill the conduit under these conditions) would have to be absent.

Conclusions

Because conduit geometry and rock strength are not well known, it is impossible to state absolutely that groundwater could not have entered the conduit during some stages of the 1790 eruption. However, the conditions that allow groundwater influx should have been the exception, not the rule. As exceptional cases, one would expect them to have been brief and intermittent, perhaps limited to waning stages of a eruptive cycle. The fact that water mixed with magma constantly throughout the 1790 eruption suggests either that water pressures did not follow a normal hydrostat at Kilauea or that the water table lay above the ground surface.

Possibility of Overpressure

If an overpressured groundwater system existed in 1790, it would most likely have lain beneath an impermeable cap rock of hydrothermal minerals (deposited in a process called "self sealing" by *Facca and Tonani* [1967]). Self sealing has been attributed to pressure increases that precede hydrothermal eruptions in volcanic areas (such as Waiotapu, New Zealand [Hedenquist and Henley, 1985], and Soufriere de Guadeloupe [Zlotnicki et al., 1992]). In the 1970s a 1.2-km-deep hole was drilled a few hundred meters south of Kilauea's caldera rim to search for a sealed hydrothermal system [Keller et al., 1979]. That study found no evidence of high pressures. Moreover, no extensive mineralized zones were found at shallow depth that could have represented a seal of an earlier system. On the basis of temperature logs of the hole and on thermal models, *Keller et al.* [1979] inferred that groundwater within a few hundred meters of the water table (at 488-m depth) was actively connecting within an unconfined aquifer of moderate to high per-

meability (10^{-13} – 10^{-14} m²). At greater depth, increasing temperatures suggested that heat flow was increasingly dominated by conduction caused by decreasing permeability. If a sealed, overpressured hydrothermal system exists at the summit of Kilauea, it apparently lies below 1.2-km depth.

Evidence for a Caldera Lake

From the geologic record we know that the 1790 eruption was preceded about 2100 ¹⁴C years ago by major hydromagmatic eruptions from an earlier summit caldera [Dzurisin et al., 1995]. The last of those eruptions was immediately followed by rapid caldera infilling [Powers, 1948; Dzurisin et al., 1995] and then by growth of a lava shield at the summit [Holcomb, 1987]. The present caldera began to form sometime after the late 1600s (D. Clague, personal communication, 1995) but before the 1790 eruption, as some faults that bound the caldera are draped by unbroken layers of Keanakakoi Ash (R. L. Christiansen, USGS, personal communication, 1996).

The 1790 eruption, like its hydromagmatic predecessor, was followed by rapid caldera infilling which continued until it reached its approximate, present-day elevation by the 1890s [MacDonald et al., 1983, p. 71–79]. In the early 1800s, when the first observations were recorded, infilling was rapid and was interrupted by episodes of magma withdrawal associated with rift zone eruptions. One such episode took place a few weeks before the arrival of the first Europeans in August 1823 [Ellis, 1827]. During that first visit the elevation of the caldera floor prior to withdrawal was visible as a Black Ledge around the caldera, several hundred feet above its floor. William Ellis, the leader of that group, estimated the caldera's depth as [Ellis, 1827, p. 176] "not less than 700 or 800 feet." Another member of the group estimated it at [Ellis, 1827, p. 176] "not less than one thousand feet," and added, "We had good opportunities for forming [such] a judgment." In each case they judged the crater depth above the Black Ledge to be roughly equal to that below.

When the first map of the caldera was surveyed in 1825, Charles Malden, head of the mapping project, measured the caldera floor depth from a survey point at Byron Ledge on the east side (Figure 1). His account follows [Byron, 1827, p. 184]:

A short base-line was measured, and some of the most conspicuous points of the volcano fixed by triangulation, from which it appears that the circumference of the crater is nearly eight miles; the distance from that hut [at Byron Ledge] to the cliff marked no. 7 in the plan [Uwekahuna Bluff] was found to be 8,207 feet, and the angle subtended between the top and bottom of the cliff 5°55'; this will give 932 feet perpendicular to the Black Ledge, to which add 400 feet, the estimated height of the Black Ledge above the bottom of the crater. I am convinced this measurement is within 100 feet of the truth.

Malden used an incorrect value for the sine of 5°55' and a distance to Uwekahuna bluff that was significantly less than that shown on current maps (~9100 feet or ~2774 m). Correcting these values gives a vertical distance to the Black Ledge of about 938 feet (286 m) and a total depth of approximately 1340 feet (408 m). Using an elevation of 4030 feet (1228 m) at the top of Uwekahuna Bluff, this would give an elevation at the bottom of the crater of roughly 2690 feet or 820 m above sea level.

After hearing of Malden's measurement one member of Ellis's party [Goodrich, 1829] recognized that their group had underestimated the caldera floor depth by nearly a factor of 2. He later estimated the depth of the inner crater in 1823 to have been about 850 feet [Goodrich, 1833], making the total depth

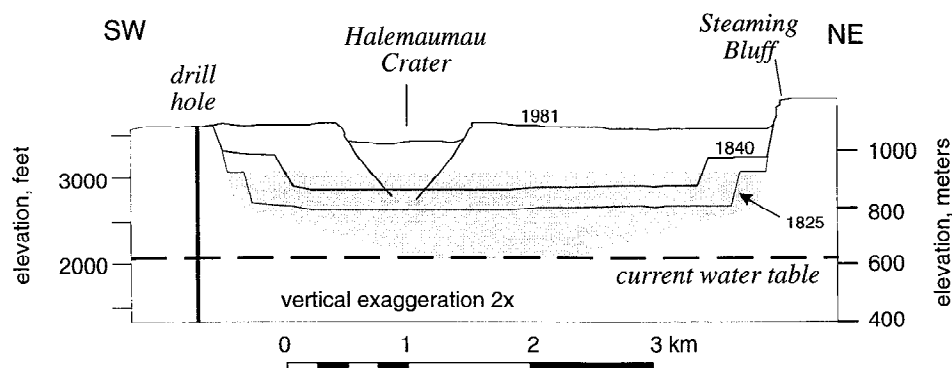


Figure 11. Profiles of Kilauea Caldera in 1825, 1840, and 1981 (from the current 7.5 arc min USGS topographic map). Location of the profile in map view is shown in Figure 1. Profiles of 1825 and 1840 are based on maps made during those years [Byron, 1827; Wilkes, 1845; Fitzpatrick, 1986]. The water table depth is taken from the drill hole [Keller et al., 1979]. This depth is considered conservative, as geophysical surveys [Kauahikaua, 1993] suggest that the water table rises toward the northeast side of the caldera, perhaps to an elevation of 800 m. The shaded area is explained in the text.

in 1823 more than 1790 feet (540 m) and leaving the crater floor less than 200 feet (60 m) above the current water table.

Between 1825 and 1832 the caldera filled to an elevation about 50 feet (15 m) above the Black Ledge [Goodrich, 1833]. During an eruption in late 1832 it drained back nearly to the level of 1823 [Goodrich, 1833] and then filled to a new high mark by 1840, after which another eruption produced a new, smaller inner crater. In late 1840 the U.S. Exploring Expedition, under the command of Charles Wilkes [Wilkes, 1845] mapped the caldera and recorded a depth of 650 feet (198 m) from the crater rim at Uwekahuna Bluff to the Black Ledge and 342 feet (104 m) from that point to the caldera floor [Wilkes, 1845; Fitzpatrick, 1986, p. 94].

On the basis of these maps and estimates of caldera depth, I estimate infilling rates of $0.13\text{--}0.48\text{ km}^3\text{ yr}^{-1}$ for time periods between withdrawal episodes (see the appendix). From 1825 to 1840, which includes two major withdrawal episodes, the net infill rate was about $0.09\text{--}0.12\text{ km}^3\text{ yr}^{-1}$, without including the magma withdrawn from the caldera in 1832 and 1840. These rates are up to a few times greater than the average magma supply rate during the twentieth century ($\sim 0.09\text{ km}^3\text{ yr}^{-1}$) [Dvorak and Dzurisin, 1993]. The high supply rates were probably in response to a major caldera withdrawal episode in 1790. Extrapolating the trends of the early 1800s back in time, magma supply rates between 1790 and 1823 were probably higher still.

How great would the infilling rate have to have been in order to raise the caldera floor depth from an elevation below the water table in 1790 to the value observed in 1823? The total fill may have been roughly that represented by the lightly shaded area in Figure 11. I calculate the volume of this area in two sections, using the formula for the frustum of a right circular cone (i.e., a cone with its tip sliced off) for each section:

$$V = \frac{1}{3}z(A_1 + A_2 + \sqrt{A_1A_2}) \quad (14)$$

A_1 and A_2 are the areas of the top and bottom surfaces, and z is the height of the section. Using an area for the upper surface (9.85 km^2) from Table A1 and diameters d of the lightly shaded region at 800-m elevation (the break in slope) and 612-m elevation (the water table) measured from Figure 11, I calculate a total volume of 2.095 km^3 , requiring an infill rate of approximately $0.063\text{ km}^3\text{ yr}^{-1}$ between 1790 and 1823.

Clearly, this rate of infilling was possible given the rates estimated between 1825 and 1840.

Revised Eruptive Sequence

In view of the evidence presented in this paper, I propose the following revised sequence to the 1790 eruptions (Figure 12).

1. Initially, the caldera floor lay above the water table (Figure 12a). High lava fountains during that time produced a reticulite layer (unit I). The caldera subsided below the water table sometime thereafter. The absence of lake sediments in the unit II deposits and the lack of soil development or weathering of the unit I deposit prior to deposition of unit II suggest that the lake existed for a relatively short time (weeks to years?) prior to the hydromagmatic unit II eruption.

2. Eruptions through surface water fragmented the magma and produced tephra fall and surge beds (Figure 12b, unit II). Some eruptive phases involved vigorous, sustained magma ejection, though none were sufficiently vigorous to dry out the vent.

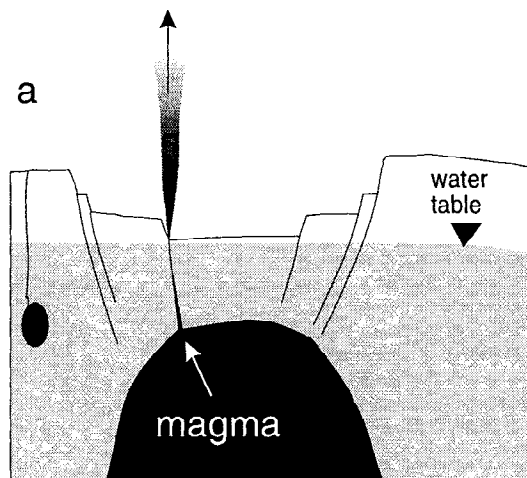
3. Continued subsidence of the caldera produced rockfalls and landslides that periodically blocked the vent with lithic debris (Figure 12c). Pressure buildup within the blocked vent was released during discrete explosions that generated extensive base surges and ejected both juvenile and lithic debris (unit III). Subsidence was also sufficient to open circumferential fissures outside the caldera margin, some of which provided pathways for lava flows (unit IV).

4. Continued subsidence, accompanied by rockfall and landslides, eventually blocked the vent, but explosions continued as hot lithic debris from the crater walls collapsed and mixed with surface water or groundwater (Figure 12d, unit V).

5. Eventually, perhaps over years or decades, the caldera floor rose above the water table and lava fountains (unit VI) erupted without water interaction.

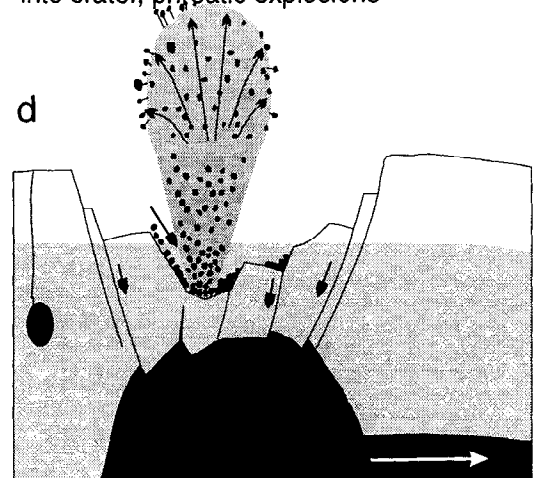
This sequence differs from that of previous authors primarily in its consideration of a lake in the caldera during eruption of units II–V. It also differs from Figure 9 of McPhie et al. [1990] in two respects: (1) it envisions sustained magma ascent during certain phases of the unit II eruption, rather than exclusively repeated, discrete explosions; (2) it shows the sequence accompanied by subsidence of the entire caldera, rather than by magma withdrawal and conduit collapse in the immediate vent area. Subsidence of the entire caldera was

UNIT I: fountaining, no groundwater influx



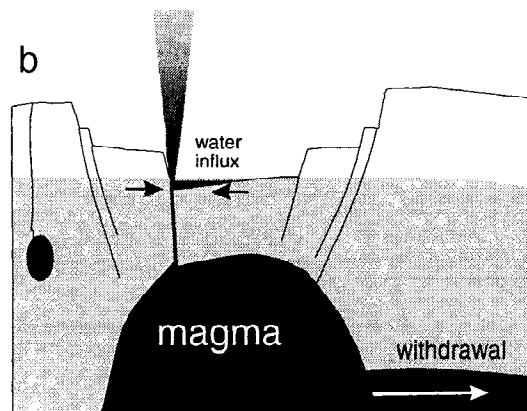
pause, subsidence of caldera below water table

UNIT V: massive slumping and landsliding into crater, phreatic explosions

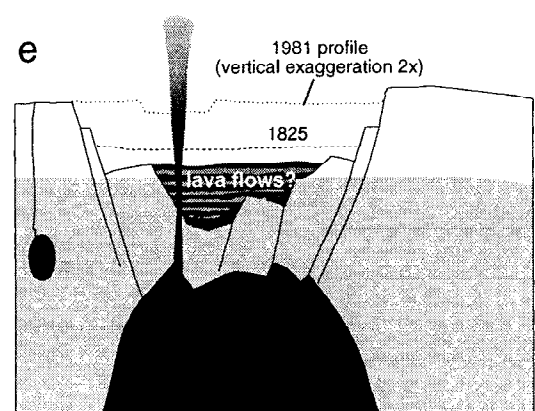


long pause (decades?), buildup of caldera floor above water table

UNIT II: repeated, sometimes vigorous eruptions through shallow water



UNIT VI: high lava fountains, no water influx



UNITS III & IV: collapse of vent and crater walls, periodic vent blockage, massive, episodic explosions, fissure eruptions nearby

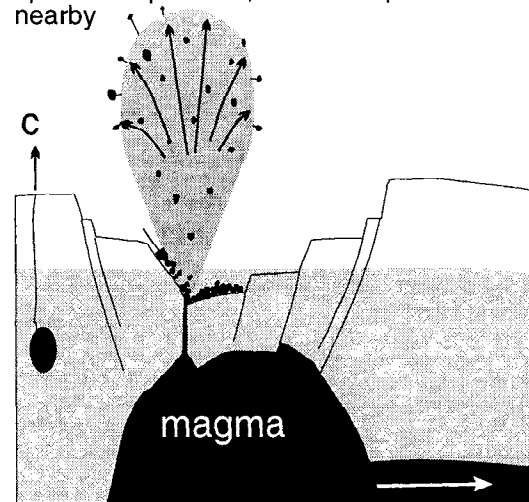


Figure 12. Sequence of events envisioned for the 1790 eruptions, revised from previous authors according to the considerations presented in this paper.

Table A1. Depth and Surface Area of Kilauea Caldera and Its Inner Craters Taken From Contemporary Observations

Feature	Elevation, m						Area, km ²					
	1823 Early August	1825 Late June	1832 Early January	1832 Mid- January	1840 Late May	1840 Late June	1823 Early August	1825 Late June	1832 Early January	1832 Mid- January	1840 Late May	1840 Late June
Caldera rim	1225 ^a	1225	1225	1225	1225	1225	12.18 ^b	12.18	12.18	12.18	12.18	12.18
Outer margin of Black Ledge	940 ^c	940	955 ^d	955	1027 ^e	1027	9.85	9.85	9.85	9.85	8.13	8.13
Inner margin of Black Ledge	940	940	...	955	...	1027	6.23–8.83 ^f	6.23–8.83 ^g	...	6.23–8.83 ^h	3.42	
Crater floor	681 ⁱ	818 ^j	...	681 ^k	...	923 ^l	3.78–5.86 ^m	5.00–7.35 ⁿ	...	3.78–5.86 ^o	...	1.18

^aPresent elevation of the highest point at Uwekahuna Bluff. The elevation of this point has remained essentially unchanged since 1823.

^bEquals the present-day area within the caldera rim. This area has not changed significantly since 1823.

^cThe elevation of Uwekahuna Bluff minus the depth to the Black Ledge (938 feet) from Malden’s measurement but corrected using the true horizontal distance from Byron Ledge to Uwekahuna Bluff (9100 feet) and the correct sine of 5°55’.

^dGoodrich [1833, p. 202] noted that prior to an eruption in January 1832, “The crater had been filled up to the Black Ledge and about fifty feet above it” since his first visit in 1823. This value is therefore 50 feet (15 m) higher than the 1825 elevation.

^eThe elevation at Uwekahuna Bluff, minus the depth to the Black Ledge (650 feet) measured by the Wilkes mapping party in 1840.

^fAssumed to be the same as in 1825.

^gThe larger value was obtained from Malden’s map. However, in 1823, members of Ellis’s party measured the circumference of the rim of the inner crater with a line and found it to be [Ellis, 1827, p. 176] “at least five miles and a half.” The smaller value therefore represents the area of a circle 5.5 miles (8.851 km) in circumference.

^hAssumed to be equal to the area within the inner margin of the Black Ledge of 1825.

ⁱGoodrich [1833].

^jThe elevation of the Black Ledge minus the 400-foot depth of the inner crater estimated by Malden in 1825.

^kGoodrich [1833, p. 202] noted that prior to the eruption in January, 1832, “the caldera had been filled up to the Black Ledge and about fifty feet above it, about nine hundred feet in the whole, since I first visited it [in 1823], and it had now [in September, 1832] again sunk down to nearly the same depth as at first.” The elevation given here (680 m) is therefore 900 feet lower than that of the Black Ledge.

^lThe elevation of the Black Ledge minus the depth of the inner crater (342 feet) measured by the Wilkes mapping party of 1840.

^mThe larger value was calculated by taking the area within the inner margin of the Black Ledge (8.83 km²) and of the crater floor (7.35 km²) from the 1825 map and calculating the change in the equivalent crater radius r with elevation dr/dz , where $r = (Area/\pi)^{0.5}$. The result is $dr/dz = 1.20$. The larger area (5.86 km²) was therefore calculated using the formula $5.86 \text{ km}^2 = \pi [(8.83 \text{ km}^2/\pi)^{0.5} - 1.20(0.259 \text{ km})]^2$, where 0.259 km is the depth of the crater. This calculation assumes that the slope of the crater walls was the same in the lower part of the crater as in the upper part. The smaller value (3.78 km²) was calculated in a similar way but using an area at the top of the inner crater of 6.23 km².

ⁿThe larger number is the area of the crater floor on Malden’s map. This is 0.832 times the area inside the inner Black Ledge measured from Malden’s map. The smaller number is therefore obtained by multiplying the smaller estimate for the area within the inner Black Ledge (6.23 km²) by the ratio 0.832.

^oAssumed to be equal to the area of the crater floor in 1823.

observed during drawdown events in the 1800s, which were probably smaller than that of 1790. In addition the steam blast explosions of 1924 were accompanied by subsidence and rock-fall from throughout the walls of the 1-km-diameter, 400-m-deep crater of Halemaumau [Decker and Christiansen, 1984]. The unit V Kenakakoi deposit is similar to but about 20 times more voluminous than the 1924 deposit [Decker and Christiansen, 1984; McPhie et al., 1990], suggesting a source crater that was closer to the diameter of the caldera (~3 km).

Closing Thoughts

The brief historical record in Hawaii has demonstrated that Kilauea’s caldera floor falls and rises by hundreds of meters as the caldera drains and refills. One need not extrapolate this trend very far to realize that occasional subsidence below the water table is inevitable.

The present elevation of the caldera floor, nearly 500 m above the water table, would seem to suggest a low probability

Table A2. Volume of Craters and Fills

Feature	Variable name	A ₂ , km ²	A ₁ , km ²	z, km	V, km ³
Crater fill, August 1823 to June 1825	V ₀	3.78–5.86	5.00–7.35	0.137	0.61–0.90
Inner crater, 1825	V ₁	5.00–7.35	6.23–8.83	0.122	0.68–0.99
Overflow of Black Ledge, 1832	V ₂	9.85	9.85	0.015	0.15
Inner crater in 1832 after draining	V ₃	3.78–5.86	6.23–8.83	0.274	1.35–2.00
Fill between Black Ledge of 1832 and Black Ledge of 1840	V ₄	8.13–9.85	8.13–9.85 ^a	0.087	0.71–0.86
Inner crater, 1840	V ₅	1.18	3.42	0.10	0.22

^aThe poor quality of the two maps is apparent here. Malden’s map of 1825 shows the walls of the caldera being steep around its entire circumference, whereas Wilkes’s map of 1840 shows a broad ledge on the south and west sides of the caldera, making the outer rim of the Black Ledge smaller than that shown in the 1825 map. The true map area covered by lava after it overflowed the Black Ledge of 1825 may have been something between the areas shown on the two maps. The volume calculated for this fill represents the volumes of two cylinders, one having a cross-sectional area equal to the outer margin of the Black Ledge measured by Wilkes and the other having a cross-sectional area equal to that measured by Malden.

Table A3. Calculated Volumes and Rates of Crater Fill

Time Period	Volumes Summed	Fill Volume, km ³	Time, years	Fill Rate, km ³ yr ⁻¹
1823–1825	V_0	0.61–0.90	1.88	0.32–0.48
1825–1832	$V_1 + V_2$	0.83–1.14	6.50	0.13–0.17
1832–1840 (before collapse)	$V_3 + V_4$	2.06–2.86	8.38	0.25–0.34
1825–1840 (after collapse)	$V_1 + V_2 + V_4 - V_5$	1.32–1.78	14.98	0.09–0.12

of a 1790-style hydromagmatic eruption in the near future. However, it may be naive to conclude this. In 1924, with the caldera floor at its approximate, present-day elevation, Halemaumau crater subsided to a level nearly 400 m below the surrounding caldera floor [Decker and Christiansen, 1984], ~540 m below Uwekahuna Bluff, a depth comparable to that in 1823. The steepness of the crater walls and hence the crater's final depth were controlled by the angle of repose. A crater about 20% larger in diameter than Halemaumau in 1924, with its walls at the angle of repose, would have extended below the water table. At that depth magma surges in the conduit, which were detected seismically in 1924 [Finch, 1943], could have developed into lava fountains through a caldera lake.

Appendix

Caldera fill volumes between 1825 and 1840 were estimated by multiplying areas of inundation, obtained from contemporary maps, by changes in caldera floor depth estimated or measured during that time period. Both the map of 1825 [Byron, 1827] and of 1840 [Wilkes, 1845] showed the outer margin of the caldera, the outer margin of the Black Ledge, the inner margin of the Black Ledge, and the outer margin of the flat crater floor. Those features were digitized, and the areas they encompassed calculated, in square kilometers.

Because of mapping inaccuracies, the area within the caldera margin on both maps differs from that on the current USGS 1:24,000-scale map (e.g., 12.90 km² in 1825 versus 12.18 km² currently), although the caldera margin has not changed significantly in historical time. Therefore the measured areas for 1825 were multiplied by (12.18/12.90) to give values that are perhaps more correct. A similar adjustment was made for the 1840 data. The final values are shown in Table A1. For the area within the inner rim of the Black Ledge of 1825, there is also a discrepancy between the area digitized from Malden's map and the area that one would calculate from the circumference measured by members of Ellis's party in 1823 (5.5 mi or 8.851 km) [Ellis, 1827, p. 176]. Both of these numbers are used to define a range of possible crater volumes. The methods of caldera depth estimates are explained in footnotes to Table A1.

The volumes V of the craters and crater fill were calculated using a formula for the frustum of a right circular cone (i.e., a cone with its tip sliced off):

$$V = \frac{1}{3}z(A_1 + A_2 + \sqrt{A_1A_2}) \quad (\text{A1})$$

where A_1 and A_2 are the surface areas at the top and bottom of each feature and z is its depth. Table A2 gives the volumes using this formula. The volumes of fill and fill rates during the periods 1823–1825, 1825–1832, 1832–1840, and 1825–1840 are given in Table A3.

Acknowledgments. This work has benefitted from help by several USGS coworkers. Robert Christiansen introduced me to the

Keanakakoi Ash and carefully reviewed my interpretation of it. David Clague reviewed this paper and offered additional insights into the state of the caldera in 1790. Margaret Mangan helped interpret clast vesicularity and generously analyzed vesicle size distributions. Melvin Beeson (formerly of USGS, Menlo Park) provided microprobe analyses of glass samples. Thomas Wright (formerly of USGS, Reston, Va.) pointed out the high rates of caldera infilling in the early 1800s and helped compile data for the tables in the appendix. Additional reviews of and helpful comments for this manuscript were provided by Tina Neal (USGS, Alaska), John Dvorak, Jocelyn McPhie, and Dario Tedesco.

References

- Bird, R. B., W. E. Stewart, and E. N. Lightfoot, *Transport Phenomena*, 780 pp., John Wiley, New York, 1960.
- Bottinga, Y., D. Weill, and P. Richet, Density calculations for silicate liquids, I, Revised method for aluminosilicate compositions, *Geochim. Cosmochim. Acta*, 46, 909–919, 1982.
- Byron, G., *Voyage of H.M.S. Blonde to the Sandwich Islands, in the years 1824–1825*, John Murray, London, 1827.
- Cashman, K. V., M. T. Mangan, and S. Newman, Surface degassing and modifications to vesicle size distributions in active basalt flows, *J. Volcanol. Geotherm. Res.*, 61, 45–68, 1994.
- Christiansen, R. L., Explosive eruption of Kilauea Volcano in 1790 (abstract), in *Hawaii Symposium on Intraplate Volcanism and Submarine Volcanism, Hilo, HI, July 16–22, 1979*, edited by R. W. Decker, C. Drake, G. Eaton, and C. Helsley, p. 158, U.S. Geol. Surv., Hilo, Hawaii, 1979.
- Dana, J. D., History of changes of the Mt. Loa craters, *Am. J. Sci.*, 36, 81–112, 1888.
- Decker, R. W., and R. L. Christiansen, Explosive eruptions of Kilauea volcano, Hawaii, in *Explosive Volcanism*, edited by National Research Council, pp. 122–132, Natl. Acad., Washington, D. C., 1984.
- Dibble, S., *A History of the Sandwich Islands*, 451 pp., T. G. Thrum, Lahainaluna, Hawaii, 1843.
- Dobran, F., Nonequilibrium flow in volcanic conduits and application to the eruptions of Mt. St. Helens on May 18, 1980 and Vesuvius in AD 79, *J. Volcanol. Geotherm. Res.*, 49, 285–311, 1992.
- Dvorak, J. J., Mechanism of explosive eruptions of Kilauea volcano, Hawaii, *Bull. Volcanol.*, 54, 638–645, 1992.
- Dvorak, J. J., and D. Dzurisin, Variations in magma supply rate at Kilauea volcano, Hawaii, *J. Geophys. Res.*, 98, 22,255–22,268, 1993.
- Dzurisin, D., J. P. Lockwood, T. J. Casadevall, and M. Rubin, The Uwekahuna Ash Member of the Puna Basalt: Product of violent phreatomagmatic eruptions at Kilauea volcano, Hawaii, between 2,800 and 2,100 years ago, *J. Volcanol. Geotherm. Res.*, 66, 163–184, 1995.
- Easton, M., Stratigraphy of Kilauea volcano, in *Volcanism in Hawaii*, edited by R. W. Decker et al., *U.S. Geol. Surv. Prof. Pap.*, 1350, 243–260, 1987.
- Ellis, W., *Journal of William Ellis*, 342 pp., Fisher and Jackson, London, 1827. (reprinted by the Adver. Publ., Honolulu, Hawaii, 1963.)
- Facca, G., and F. Tonani, The self-sealing geothermal field, *Bull. Volcanol.*, 30, 271–273, 1967.
- Finch, R. H., Lava surgings in Halemaumau and the explosive eruptions in 1924, *Volcano Lett.*, 479, 1–4, 1943.
- Fitzpatrick, G. L., *The Early Mapping of Hawaii*, 160 pp., Ed. Ltd., Honolulu, Hawaii, 1986.
- Gerlach, T. M., Exsolution of H₂O, CO₂, and S during eruptive episodes at Kilauea volcano, Hawaii, *J. Geophys. Res.*, 91, 12,177–12,185, 1986.
- Gerlach, T. M., and E. J. Graeber, Volatile budget of Kilauea volcano, *Nature*, 313, 273–277, 1985.
- Giberti, G., and L. Wilson, The influence of geometry on the ascent of magma in open fissures, *Bull. Volcanol.*, 52, 515–521, 1990.

- Goodrich, J., Letters from the Sandwich Islands, *Am. J. Sci.*, 16, 345-347, 1829.
- Goodrich, J., Notices of some of the volcanoes and volcanic phenomena of Hawaii, (Owyhee), and other islands in that group, *Am. J. Sci.*, 25, 199-203, 1833.
- Hedenquist, J. W., and R. W. Henley, Hydrothermal eruptions in the Waiotapu geothermal system, *Econ. Geol.*, 80, 1640-1688, 1985.
- Heiken, G., and K. Wohletz, *Volcanic Ash*, 246 pp., Univ. of Calif. Press, Berkeley, 1985.
- Helz, R. T., and C. R. Thornber, Geothermometry of Kilauea Iki lava lake, Hawaii, *Bull. Volcanol.*, 49, 651-668, 1987.
- Hitchcock, C. H., *Hawaii and Its Volcanoes*, 314 pp., Hawaiian Gazette, Honolulu, Hawaii, 1909.
- Holcomb, R. T., Eruptive history and long-term behavior of Kilauea volcano, edited by R. W. Decker, T. L. Wright, and P. H. Stauffer, *U.S. Geol. Surv. Prof. Pap.*, 1350, 261-350, 1987.
- Houghton, B. F., and C. J. N. Wilson, A vesicularity index for pyroclastic deposits, *Bull. Volcanol.*, 51, 451-462, 1989.
- Jaeger, J. C., and N. G. W. Cook, *Fundamentals of Rock Mechanics*, 593 pp., Chapman and Hall, New York, 1979.
- Jaggar, T. A., Fossil human footprints in Kau Desert, *Hawaii. Volcano Obs. Mon. Bull.*, 9, 114-118, 1921.
- Kauahikaua, J., Geophysical characteristics of the hydrothermal systems of Kilauea Volcano, Hawai'i, *Geothermics*, 22, 271-299, 1993.
- Keller, G. V., T. Grose, J. C. Murray, and C. K. Skokan, Results of an experimental drill hole at the summit of Kilauea Volcano, Hawaii, *J. Volcanol. Geotherm. Res.*, 6, 345-385, 1979.
- Kienle, J., P. R. Kyle, S. Self, R. J. Motyka, and V. Lorenz, Ukinrek Maars, Alaska, I, April 1977 eruption sequence, petrology and tectonic setting, *J. Volcanol. Geotherm. Res.*, 7, 11-37, 1980.
- Liepmann, H. W., and A. Roshko, *Elements of Gasdynamics*, 439 pp., John Wiley, New York, 1957.
- MacDonald, G. A., A. T. Abbott, and F. L. Peterson, *Volcanoes in the Sea*, 517 pp., Univ. of Hawaii Press, Honolulu, 1983.
- Mangan, M. T., and K. V. Cashman, The structure of basaltic scoria and reticulite and inferences for vesiculation, foam formation, and fragmentation in lava fountains, *J. Volcanol. Geotherm. Res.*, 73, 1-18, 1996.
- Mangan, M. T., K. V. Cashman, and S. Newman, Vesiculation of basaltic magma during eruption, *Geology*, 21, 157-160, 1993.
- Mastin, L. G., A numerical program for steady state flow of Hawaiian magma-gas mixtures through vertical eruptive conduits, *U.S. Geol. Surv. Open File Rep.*, 95-756, 46 pp., 1995. (Available at <http://vulcan.wr.usgs.gov/Projects/H2O+Volcanoes/Groundwater/frame-work.html>)
- McPhie, J., G. P. L. Walker, and R. L. Christiansen, Phreatomagmatic and phreatic fall and surge deposits from explosions at Kilauea volcano, Hawaii, 1790 A.D.: Keanakakoi Ash Member, *Bull. Volcanol.*, 52, 334-354, 1990.
- Parfitt, E. A., and L. Wilson, Explosive volcanic eruptions, IX, The transition between Hawaiian-style lava fountaining and Strombolian explosive activity, *Geophys. J. Int.*, 121, 226-232, 1995.
- Parfitt, E. A., L. Wilson, and C. A. Neal, Factors influencing the height of Hawaiian lava fountains: Implications for the use of fountain height as an indicator of magma gas content, *Bull. Volcanol.*, 57, 440-450, 1995.
- Powers, H. A., Chronology of the explosive eruptions of Kilauea, *Pac. Sci.*, 2, 278-292, 1948.
- Press, W. H., B. P. Flannery, S. A. Teukolsky, and W. T. Vetterling, *Numerical Recipes*, 818 pp., Cambridge Univ. Press, New York, 1986.
- Ryan, M. P., and J. Y. K. Blevins, The viscosity of synthetic and natural silicate melts and glasses at high temperatures and 1 bar (10^5 Pascals) pressure and at higher pressures, *U.S. Geol. Surv. Bull.*, 1764, 563 pp., 1987.
- Schlichting, H., *Boundary Layer Theory*, 7th ed., 817 pp., McGraw-Hill, New York, 1979.
- Sharp, R. P., D. Dzurisin, and M. C. Malin, An early 19th century reticulite pumice from Kilauea volcano, edited by R. W. Decker, T. L. Wright, and P. H. Stauffer, *U.S. Geol. Surv. Prof. Pap.*, 1350, 395-404, 1987.
- Stearns, H. T., and W. O. Clark, Geology and water resources of the Kau District, Hawaii, *U.S. Geol. Surv. Water Supply Pap.*, 616, 194 pp., 1930.
- Stein, D. J., and F. J. Spera, Rheology and microstructure of magmatic emulsions: Theory and experiments, *J. Volcanol. Geotherm. Res.*, 49, 157-174, 1992.
- Swanson, D. A., and R. L. Christiansen, Tragic base surge in 1790 at Kilauea volcano, *Geology*, 1, 83-86, 1973.
- Vergnolle, S., and C. Jaupart, Separated two-phase flow and basaltic eruptions, *J. Geophys. Res.*, 91, 12,842-12,860, 1986.
- Wentworth, C. K., *Ash Formations of the Island of Hawaii*, 183 pp., Hawaii Volcano Res. Assoc., Honolulu, 1938.
- Wilkes, C., *Narrative of the U.S. Exploring Expedition During the Years 1838-1842*, 231 pp., Lee and Blanchard, Philadelphia, 1845.
- Wilson, L., and J. W. I. Head, Ascent and eruption of basaltic magma on the Earth and moon, *J. Geophys. Res.*, 86, 2971-3001, 1981.
- Wilson, L., R. S. J. Sparks, and G. P. L. Walker, Explosive volcanic eruptions, IV, The control of magma properties and conduit geometry on eruption column behaviour, *Geophys. J. R. Astron. Soc.*, 63, 117-148, 1980.
- Wilson, L., E. A. Parfitt, and J. W. Head, Explosive volcanic eruptions, VIII, The role of magma recycling in controlling the behaviour of Hawaiian-style lava fountains, *Geophys. J. Int.*, 121, 215-225, 1995.
- Woods, A. W., and S. M. Bower, The decompression of volcanic jets in a crater during explosive volcanic eruptions, *Earth Planet. Sci. Lett.*, 131, 189-205, 1995.
- Zlotnicki, J., G. Boudon, and J.-L. Le Mouél, The volcanic activity of La Soufriere of Guadeloupe (Lesser Antilles): Structural and tectonic implications, *J. Volcanol. Geotherm. Res.*, 49, 91-104, 1992.

L. G. Mastin, Cascades Volcano Observatory, U.S. Geological Survey, 5400 MacArthur Boulevard, Vancouver, WA 98661. (e-mail: lgmastin@usgs.gov)

(Received December 6, 1996; revised May 1, 1997; accepted May 8, 1997.)